

**Supporting Information for:**

**Finite-Size-Corrected Rotational Diffusion**

**Coefficients of Membrane Proteins and Carbon**

**Nanotubes from Molecular Dynamics Simulations**

Martin Vögele, Jürgen Köfinger, and Gerhard Hummer\*

E-mail: gerhard.hummer@biophys.mpg.de

**Online Repository**

Simulation parameters, analysis scripts, and machine-readable results are available online at  
<https://github.com/bio-phys/rotmemdiff>.

# Details on Hydrodynamic Finite-Size Correction for Rotational Diffusion

In the main text, we showed that the hydrodynamic stream function  $\psi(x, y)$  for rotatory 2D flow in the membrane under periodic boundary conditions is approximated well by the 2D Green's function  $\varphi(x, y)$  of electrostatics in 2D. Here we give further details on the expansion of  $\varphi(x, y)$  in terms of harmonic functions with square symmetry. These expressions apply to the special case of square-shaped simulation boxes in the  $xy$  plane of the membrane, with  $L$  the width of the box. We write the Green's function as

$$\varphi(x, y) = -\ln r + \frac{\pi r^2}{2L^2} + \sum_{k \geq 4} a_k p_k(x/L, y/L) \quad (\text{S1})$$

where  $r^2 = x^2 + y^2$ . Here we defined the arbitrary constant in  $\varphi(x, y)$  so that  $\lim_{r \rightarrow 0} [\varphi(x, y) + \ln(r)] = 0$ . The lowest-order harmonic functions in the unit square  $[-1/2, 1/2]^2$  with non-zero coefficients are

$$p_4(x, y) = x^4 - 6x^2y^2 + y^4 \quad (\text{S2})$$

$$p_8(x, y) = x^8 - 28x^6y^2 + 70x^4y^4 - 28x^2y^6 + y^8 \quad (\text{S3})$$

$$p_{12}(x, y) = x^{12} - 66x^{10}y^2 + 495x^8y^4 - 924x^6y^6 + 495x^4y^8 - 66x^2y^{10} + y^{12} \quad (\text{S4})$$

$$\begin{aligned} p_{16}(x, y) = & x^{16} - 120x^{14}y^2 + 1820x^{12}y^4 - 8008x^{10}y^6 \\ & + 12870x^8y^8 - 8008x^6y^{10} + 1820x^4y^{12} - 120x^2y^{14} + y^{16} \end{aligned} \quad (\text{S5})$$

These polynomials are harmonic,  $\nabla^2 p_k(x, y) = 0$ , and have square symmetry. The coefficients  $a_k$  can be determined, e.g., by matching the  $k$ -th order derivative with respect to  $x$  of  $\varphi(x, y) + \ln r$  at  $x = y = 0$  to the analytic Lekner sum given as eq 10 by Grønbech-Jensen.<sup>1</sup> In this way, one obtains expressions for the coefficients in terms of rapidly converging sums

that evaluate to:

$$a_4 = 0.78780300 \quad (\text{S6})$$

$$a_8 = 0.53197163 \quad (\text{S7})$$

$$a_{12} = 0.32823742 \quad (\text{S8})$$

$$a_{16} = 0.25098094 \quad (\text{S9})$$

With this approximation truncated after order 4, 8, 12, and 16, the maximum absolute residuals with respect to the exact electrostatic Green's function  $\varphi(x, y)$  in the corners of the square,  $x = y = 1/2$ , are 0.029, 0.0043, 0.00082, and 0.00016, respectively.

As explained in the main text, the lines  $\psi(x, y) = c\varphi(x, y)$  define the stream lines of the hydrodynamic flow field, with  $c$  a constant defined by the boundary condition on the rotating cylinder. A possible concern is that  $\varphi(x, y)$  is not strictly constant on any circle with finite radius. Therefore, we determined the maximum difference of  $\varphi(x, y)$  from the mean value  $\langle \varphi \rangle_\theta$  along circles of different radii using the Lekner sums given by Grønbech-Jensen.<sup>1</sup> For hydrodynamic radii  $R_H = L/10$ ,  $L/5$ , and  $L/3$ , we found maximum relative differences  $\max_\theta |\varphi(\cos \theta, \sin \theta) - \langle \varphi \rangle_\theta| / \langle \varphi \rangle_\theta$  of 0.0035 %, 0.075 %, and 0.76 %. We conclude that even for relatively large cylinder radii, the deviations are small.

# Analysis of the Mean Squared Displacement

In the following, we explore if and when a regime of regular diffusion has been reached. We first use the dilute systems to estimate the linear regime from log-log plots and to compare the linear fits to a coupled-diffusion model. We then confirm our results for both dilute and constant-density simulations via additional fits at a later lag time interval.

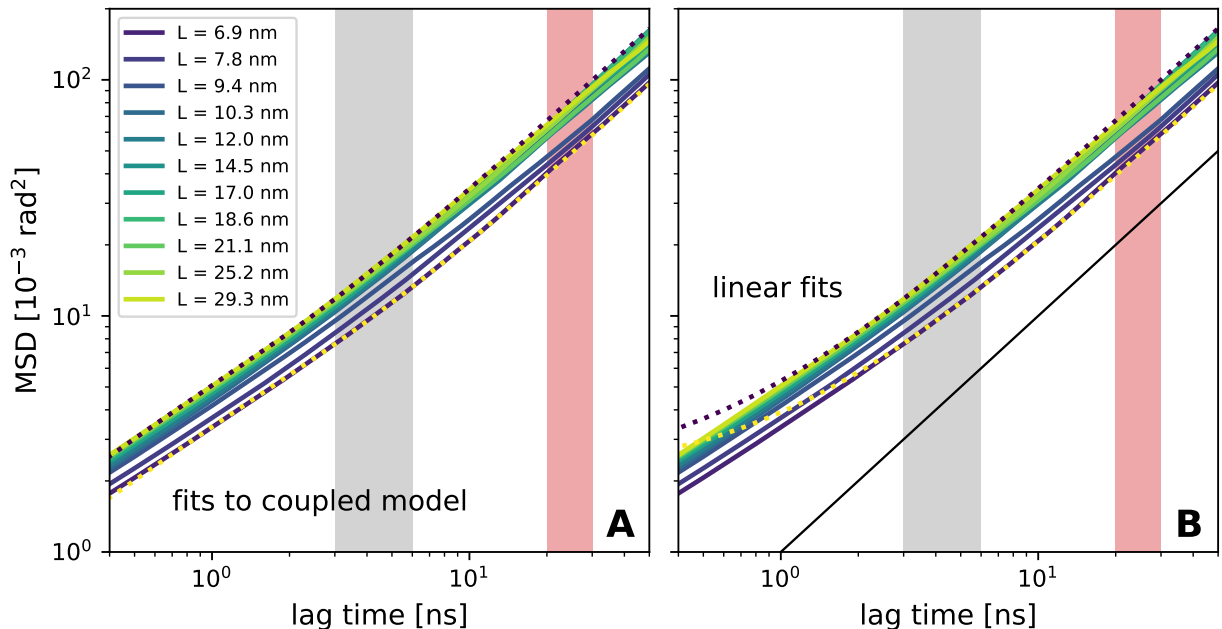


Figure S1: Mean squared displacement (MSD) of ANT1 rotation as a function of lag time  $t$  in simulations of dilute systems with one protein in the membrane. The fit range from  $t = 3$  ns to  $6$  ns used in the main text is shaded in gray and the range from  $t = 20$  ns to  $30$  ns used for an additional analysis is shaded in red. **(A)** Dotted lines show fits to the coupled-diffusion model eq S10 over the time window of  $0\text{-}7$  ns for the largest box (blue dots) and the smallest box (yellow dots). **(B)** Dotted lines show linear fits,  $MSD(t) = 2Dt + a$ , over the time window of  $3\text{-}6$  ns (gray). Note that the linear relations appear bent in the logarithmic representation due to the offset. The black line indicates a linear relation without offset.

**Linear Regime of the MSD.** To assess when a linear regime of regular diffusion has been reached, we show the MSD curves in a log-log representation (Figure S1). The initial spread in orientation resulting from fast molecular-scale dynamics leads to deviations from regular diffusion,  $MSD(t) = 2Dt$ , instead exhibiting apparent sub-diffusive behavior,  $MSD(t) \approx ct^\alpha$

with  $\alpha < 1$  and  $c > 0$ . However, as shown in Figure S1 B, adding a simple offset,  $\text{MSD}(t) = 2Dt + a$ , accounts well for the dynamics after  $t \approx 2$  ns.

**Model for Coupled Diffusion.** In an effort to account for the MSD curves also in the initial non-linear phase (but outside the ballistic regime), we considered a model of harmonically coupled diffusion. Specifically, we assumed overdamped Langevin dynamics of the apparent rotation angle  $\theta$  with a diffusion coefficient  $D_1$ , and of a hidden angle  $\gamma$  with diffusion coefficient  $D_2$ . One can think of  $\gamma$  as the orientation preferred by the slowly relaxing membrane environment, and of  $\theta$  as the actual orientation. In this model,  $\theta$  and  $\gamma$  are harmonically coupled by a potential  $k(\theta - \gamma)^2/2$  with  $k$  the spring constant in units of  $k_{\text{B}}T$ . For this model, the apparent MSD of  $\theta$ , averaged over the hidden dynamics of  $\gamma$ , is

$$\text{MSD}(t) = 2 \left[ \frac{t}{1/D_1 + 1/D_2} + \frac{1 - \exp[-k(D_1 + D_2)t]}{k(1 + D_2/D_1)^2} \right] + a \quad (\text{S10})$$

with a small added offset  $a$  accounting for the earliest dynamics. At short times,  $0 < k(D_1 + D_2)t \ll 1$ ,  $\theta$  diffuses “freely” with diffusion coefficient  $D_1$ ; at long times,  $k(D_1 + D_2)t \gg 0$ , the apparent friction coefficient acting on  $\theta$  is the sum of the friction coefficients on  $\theta$  and  $\gamma$ , resulting in an apparent diffusion coefficient  $D_{\text{lim}} = 1/(1/D_1 + 1/D_2)$ ; at intermediate times, the dynamics transitions from free to coupled diffusion.

We fitted all MSD curves of the dilute systems over the entire time window from 0 to 7 ns to eq S10, giving us the individual diffusion coefficients  $D_1$  and  $D_2$  as well as the limiting diffusion coefficient  $D_{\text{lim}}$  for large lag times. The resulting fits describe the MSD almost perfectly as indicated by the two example curves in Figure S1. The average offset is  $a = 2.4(6) \times 10^{-4} \text{ rad}^2$  and the average coupling constant is  $k = 292(55) \text{ rad}^{-2}$ .

We compared the resulting  $D_{\text{lim}}$  to the diffusion coefficient  $D$  from linear fits in the range from 3 ns to 6 ns. As shown in Figure S2,  $D_{\text{lim}}$  and  $D$  agree well, with the average deviation being 0.13% and the largest deviation being 1.68%. This indicates that the chosen fitting range of the linear fits is already representative for the long-time behavior of the MSD.

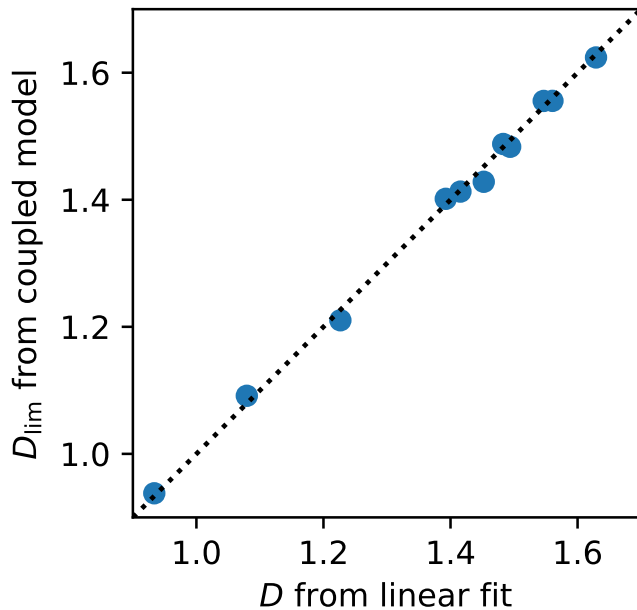


Figure S2: Comparison of the diffusion coefficients from linear fits in the range 3 ns to 6 ns to the long-time limiting values for diffusion coefficients from fits to the model of harmonically coupled diffusion, eq S10, in the range 0 ns to 7 ns. Results are for ANT1 rotational diffusion in simulations with a single ANT1 protein in the membrane at different box widths.

Interestingly, all three diffusion coefficients from the coupled model follow the size dependence eq 15 from our hydrodynamic theory (Figure S3). This result implies that the hydrodynamic finite-size correction applies to both the short time diffusion  $D_1$ , the hidden diffusion  $D_2$ , and the effective coupled diffusion  $D_{\text{lim}} = 1/(1/D_1 + 1/D_2)$ . Hydrodynamic interactions thus appear to impact the dynamics at all relevant time scales.

**Fitting MSDs at Long Times.** As a test of the dependence on the fit range, we repeated the analysis of the main text using linear fits of the MSD curves over the time window from 20 ns to 30 ns. In this window, a fit of an anomalous diffusion model with an offset,  $\text{MSD}(t) = ct^\alpha + a$ , gives an exponent  $\alpha = 0.96(5)$  statistically indistinguishable from 1. This value was obtained by averaging the fit coefficients for the different dilute ANT1 systems. Figure S4 shows the resulting diffusion coefficients as a function of box width for systems with a single ANT1 protein and with ANT1 proteins at constant concentration. From fits of eq 15,

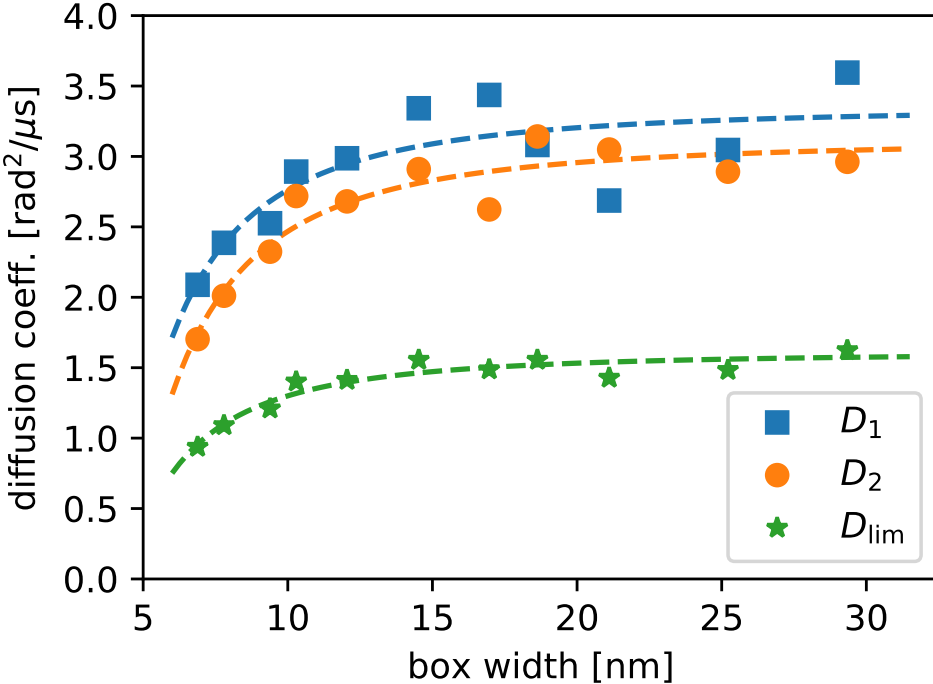


Figure S3: Diffusion coefficients from fits to the coupled-diffusion model eq S10. Dashed lines in the corresponding colors show fits to the hydrodynamic box-size dependence eq 23.

we obtained the same hydrodynamic radius as for the standard analysis ( $R_H = 2.5(2)$  nm), a slightly lower diffusion coefficient  $D_0 = 1.53 \text{ rad}^2/\mu\text{s}$  (compared to  $1.63 \text{ rad}^2/\mu\text{s}$  for the window of 3-6 ns), and a slightly higher membrane surface viscosity  $\eta_m = 3.49 \times 10^{-11} \text{ Pa s m}$  (compared to  $3.28 \times 10^{-11} \text{ Pa s m}$ ). Importantly, the general trends are preserved, even though the individual  $D$  values scatter more widely (compare Figure 3 in the main text and Figure S4).

In the constant-density simulations, we do not have as good sampling. As a result, the fits to the 20-30 ns window of the MSD curves result in relatively large statistical errors. We obtain a hydrodynamic radius  $R_H = 2.9(6)$  nm consistent with the value of the main analysis,  $R_H = 2.3(2)$  nm, but with a large uncertainty; a diffusion coefficient of  $D_0 = 1.42 \text{ rad}^2/\mu\text{s}$  (compared to  $1.47 \text{ rad}^2/\mu\text{s}$ ); and a membrane viscosity of  $\eta_m = 2.87 \times 10^{-11} \text{ Pa s m}$  (compared to  $3.28 \times 10^{-11} \text{ Pa s m}$ ).

In light of the results for concentrated and dilute ANT1 membrane systems, we conclude

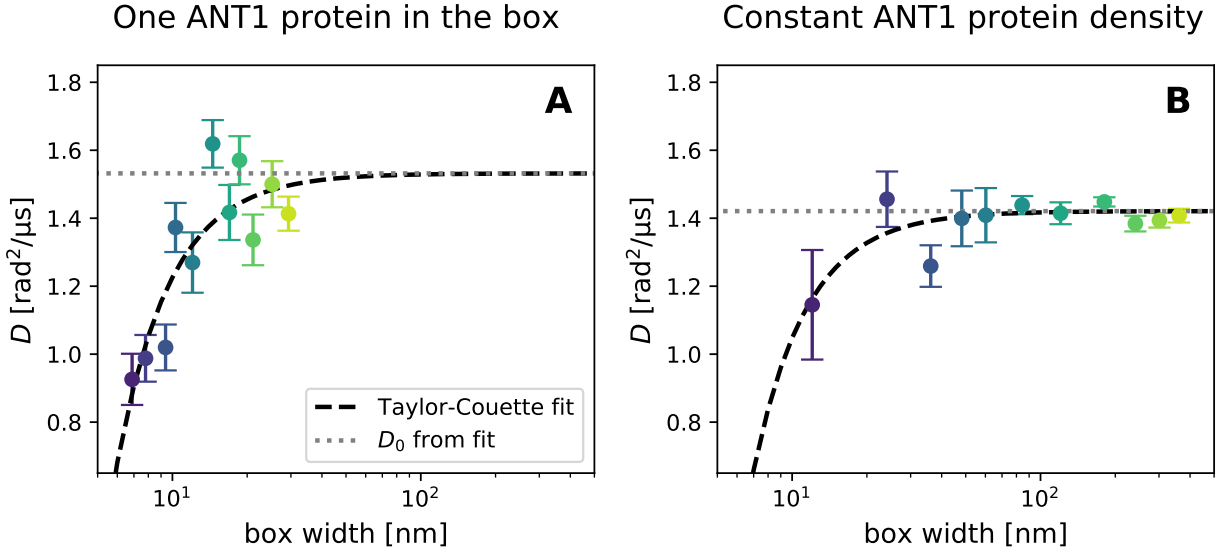


Figure S4: Box-width dependence of the rotational diffusion coefficients of ANT1 proteins in lipid membranes from linear fits to  $\text{MSD}(t)$  between 20 ns and 30 ns. **(A)** Diffusion coefficients from MD simulations of systems containing one protein per simulation box (symbols) with fit (dashed line) to hydrodynamic theory and infinite-system value  $D_0$  (dotted line) obtained from this fit. **(B)** Diffusion coefficients from MD simulations of systems containing ANT1 proteins at constant area density with the corresponding fit. Error bars denote 1 SE.

that the analysis at the earlier regime, from 3 to 6 ns, offers a good tradeoff between small systematic errors (because the asymptotic regime of regular diffusion has practically been reached) and small statistical errors (because the scatter in the MSD increases substantially at longer times). Most importantly, the finite-size effects on rotational diffusion are robust, independent of the fitting range, as can be seen by comparing Figure 3 of the main text and Figure S4.

# Simulation Details

Table 1: Simulation details for boxes narrower than 15 nm.

initial width [nm]	number POPC	number POPE	number cardiolipin	number water	average width [nm]	average height [nm]	simulation time [ $\mu$ s]	rotational diffusion coefficient [ $\text{rad}^2/\mu\text{s}$ ]
7	60	43	5	2308	$6.88 \pm 0.05$	$10.67 \pm 0.14$	2.00	$0.91 \pm 0.07$
7	60	43	5	2307	$6.88 \pm 0.05$	$10.66 \pm 0.14$	2.00	$0.87 \pm 0.09$
7	60	43	5	2305	$6.88 \pm 0.05$	$10.66 \pm 0.14$	2.00	$0.98 \pm 0.08$
7	60	43	5	2305	$6.88 \pm 0.04$	$10.66 \pm 0.14$	2.00	$0.89 \pm 0.07$
7	60	43	5	2306	$6.88 \pm 0.05$	$10.66 \pm 0.14$	2.00	$0.92 \pm 0.10$
7	60	43	5	2310	$6.88 \pm 0.05$	$10.67 \pm 0.14$	2.00	$1.02 \pm 0.07$
8	82	59	7	2996	$7.80 \pm 0.05$	$10.73 \pm 0.13$	2.00	$1.17 \pm 0.10$
8	82	59	7	3000	$7.79 \pm 0.05$	$10.76 \pm 0.13$	2.00	$0.95 \pm 0.07$
8	82	59	7	2995	$7.79 \pm 0.05$	$10.74 \pm 0.13$	2.00	$1.04 \pm 0.13$
8	82	59	7	2995	$7.79 \pm 0.05$	$10.74 \pm 0.13$	2.00	$1.26 \pm 0.10$
8	82	59	7	3000	$7.80 \pm 0.05$	$10.75 \pm 0.13$	2.00	$0.99 \pm 0.11$
8	82	59	7	2994	$7.79 \pm 0.05$	$10.73 \pm 0.13$	2.00	$1.07 \pm 0.09$
9	127	92	11	3756	$9.39 \pm 0.05$	$9.82 \pm 0.10$	2.00	$1.32 \pm 0.13$
9	127	92	11	3753	$9.39 \pm 0.05$	$9.82 \pm 0.10$	2.00	$1.02 \pm 0.12$
9	127	92	11	3758	$9.38 \pm 0.05$	$9.83 \pm 0.10$	2.00	$1.39 \pm 0.10$
9	127	92	11	3752	$9.39 \pm 0.05$	$9.82 \pm 0.10$	2.00	$1.23 \pm 0.07$
9	127	92	11	3750	$9.39 \pm 0.05$	$9.81 \pm 0.10$	2.00	$1.19 \pm 0.11$
9	127	92	11	3750	$9.39 \pm 0.05$	$9.82 \pm 0.10$	2.00	$1.21 \pm 0.10$
10	156	113	14	4614	$10.29 \pm 0.05$	$9.95 \pm 0.10$	2.00	$1.50 \pm 0.12$
10	156	113	14	4610	$10.29 \pm 0.05$	$9.94 \pm 0.10$	2.00	$1.11 \pm 0.07$
10	156	113	14	4617	$10.29 \pm 0.05$	$9.95 \pm 0.10$	2.00	$1.36 \pm 0.15$
10	156	113	14	4605	$10.29 \pm 0.05$	$9.94 \pm 0.10$	2.00	$1.45 \pm 0.11$
10	156	113	14	4611	$10.29 \pm 0.05$	$9.95 \pm 0.09$	2.00	$1.56 \pm 0.14$
10	156	113	14	4620	$10.29 \pm 0.05$	$9.96 \pm 0.10$	2.00	$1.38 \pm 0.09$
12	220	160	20	6590	$12.05 \pm 0.05$	$10.20 \pm 0.09$	2.00	$1.49 \pm 0.13$
12	220	160	20	6591	$12.05 \pm 0.05$	$10.20 \pm 0.09$	2.00	$1.54 \pm 0.16$
12	220	160	20	6586	$12.05 \pm 0.05$	$10.19 \pm 0.09$	2.00	$1.19 \pm 0.09$
12	220	160	20	6588	$12.05 \pm 0.05$	$10.19 \pm 0.09$	2.00	$1.41 \pm 0.11$
12	220	160	20	6587	$12.05 \pm 0.05$	$10.20 \pm 0.09$	2.00	$1.40 \pm 0.11$
12	220	160	20	6582	$12.05 \pm 0.05$	$10.18 \pm 0.09$	2.00	$1.46 \pm 0.09$
14	328	238	30	8893	$14.53 \pm 0.05$	$9.74 \pm 0.07$	2.00	$1.69 \pm 0.19$
14	328	238	30	8890	$14.53 \pm 0.05$	$9.74 \pm 0.07$	2.00	$1.52 \pm 0.09$
14	328	238	30	8890	$14.53 \pm 0.05$	$9.74 \pm 0.07$	2.00	$1.41 \pm 0.09$
14	328	238	30	8885	$14.53 \pm 0.05$	$9.74 \pm 0.07$	2.00	$1.55 \pm 0.11$
14	328	238	30	8900	$14.53 \pm 0.05$	$9.75 \pm 0.07$	2.00	$1.55 \pm 0.11$
14	328	238	30	8890	$14.53 \pm 0.05$	$9.74 \pm 0.07$	2.00	$1.55 \pm 0.16$

Table 2: Simulation details for boxes wider than 15 nm.

initial width [nm]	number POPC	number POPE	number cardiolipin	number water	average width [nm]	average height [nm]	simulation time [ $\mu$ s]	rotational diffusion coefficient [ $\text{rad}^2/\mu\text{s}$ ]
16	456	330	41	11534	$16.96 \pm 0.05$	$9.47 \pm 0.06$	2.00	$1.45 \pm 0.14$
16	456	330	41	11534	$16.96 \pm 0.05$	$9.47 \pm 0.06$	2.00	$1.45 \pm 0.10$
16	456	330	41	11535	$16.96 \pm 0.05$	$9.47 \pm 0.06$	2.00	$1.42 \pm 0.13$
16	456	330	41	11535	$16.96 \pm 0.05$	$9.47 \pm 0.06$	2.00	$1.35 \pm 0.09$
16	456	330	41	11533	$16.97 \pm 0.05$	$9.46 \pm 0.06$	2.00	$1.64 \pm 0.12$
16	456	330	41	11540	$16.96 \pm 0.05$	$9.47 \pm 0.06$	2.00	$1.60 \pm 0.16$
18	553	401	50	14534	$18.63 \pm 0.05$	$9.71 \pm 0.05$	2.00	$1.71 \pm 0.13$
18	553	401	50	14544	$18.63 \pm 0.05$	$9.71 \pm 0.05$	2.00	$1.63 \pm 0.17$
18	553	401	50	14550	$18.63 \pm 0.05$	$9.72 \pm 0.06$	2.00	$1.35 \pm 0.18$
18	553	401	50	14546	$18.63 \pm 0.05$	$9.72 \pm 0.05$	2.00	$1.77 \pm 0.17$
18	553	401	50	14548	$18.63 \pm 0.05$	$9.72 \pm 0.06$	2.00	$1.34 \pm 0.11$
18	553	401	50	14542	$18.63 \pm 0.05$	$9.71 \pm 0.05$	2.00	$1.56 \pm 0.18$
20	713	520	65	17856	$21.11 \pm 0.05$	$9.46 \pm 0.05$	2.00	$1.48 \pm 0.13$
20	713	520	65	17857	$21.11 \pm 0.05$	$9.46 \pm 0.05$	2.00	$1.27 \pm 0.14$
20	713	520	65	17860	$21.11 \pm 0.05$	$9.46 \pm 0.05$	2.00	$1.35 \pm 0.11$
20	713	520	65	17867	$21.11 \pm 0.05$	$9.47 \pm 0.05$	2.00	$1.48 \pm 0.09$
20	713	520	65	17866	$21.11 \pm 0.05$	$9.47 \pm 0.05$	2.00	$1.62 \pm 0.23$
20	713	520	65	17865	$21.11 \pm 0.05$	$9.47 \pm 0.05$	2.00	$1.51 \pm 0.17$
24	1028	746	93	25577	$25.22 \pm 0.05$	$9.48 \pm 0.04$	2.00	$1.44 \pm 0.10$
24	1028	746	93	25564	$25.22 \pm 0.05$	$9.48 \pm 0.04$	2.00	$1.44 \pm 0.11$
24	1028	746	93	25561	$25.22 \pm 0.05$	$9.48 \pm 0.04$	2.00	$1.34 \pm 0.09$
24	1028	746	93	25561	$25.22 \pm 0.05$	$9.48 \pm 0.04$	2.00	$1.56 \pm 0.13$
24	1028	746	93	25570	$25.22 \pm 0.05$	$9.48 \pm 0.04$	2.00	$1.52 \pm 0.09$
24	1028	746	93	25563	$25.22 \pm 0.05$	$9.48 \pm 0.04$	2.00	$1.66 \pm 0.15$
28	1396	1016	127	34623	$29.34 \pm 0.05$	$9.48 \pm 0.03$	2.00	$1.58 \pm 0.16$
28	1396	1016	127	34623	$29.34 \pm 0.05$	$9.48 \pm 0.03$	2.00	$1.95 \pm 0.11$
28	1396	1016	127	34614	$29.35 \pm 0.05$	$9.48 \pm 0.03$	2.00	$1.40 \pm 0.08$
28	1396	1016	127	34635	$29.34 \pm 0.05$	$9.48 \pm 0.03$	2.00	$1.64 \pm 0.15$
28	1396	1016	127	34642	$29.34 \pm 0.05$	$9.48 \pm 0.03$	2.00	$1.64 \pm 0.14$
28	1396	1016	127	34632	$29.34 \pm 0.05$	$9.48 \pm 0.03$	2.00	$1.56 \pm 0.08$

Table 3: Simulation details of the height study.

initial width [nm]	initial height [nm]	number POPC	number POPE	number cardiolipin	number water	average width [nm]	average height [nm]	simulation time [ $\mu$ s]	rotational diffusion coefficient [ $\text{rad}^2/\mu\text{s}$ ]
7.00	7.50	60	43	5	1090	$6.87 \pm 0.05$	$7.17 \pm 0.10$	2.00	$1.01 \pm 0.14$
7.00	7.50	60	43	5	1090	$6.87 \pm 0.05$	$7.17 \pm 0.09$	2.00	$0.85 \pm 0.05$
7.00	7.50	60	43	5	1094	$6.87 \pm 0.04$	$7.18 \pm 0.09$	2.00	$0.89 \pm 0.10$
7.00	7.50	60	43	5	1090	$6.87 \pm 0.05$	$7.17 \pm 0.09$	2.00	$1.07 \pm 0.08$
7.00	7.50	60	43	5	1088	$6.87 \pm 0.05$	$7.17 \pm 0.09$	2.00	$0.88 \pm 0.09$
7.00	7.50	60	43	5	1088	$6.87 \pm 0.05$	$7.17 \pm 0.09$	2.00	$0.95 \pm 0.10$
7.00	10.00	60	43	5	2302	$6.88 \pm 0.05$	$10.65 \pm 0.14$	2.00	$0.97 \pm 0.10$
7.00	10.00	60	43	5	2310	$6.88 \pm 0.05$	$10.67 \pm 0.14$	2.00	$0.85 \pm 0.08$
7.00	10.00	60	43	5	2305	$6.88 \pm 0.05$	$10.65 \pm 0.14$	2.00	$0.94 \pm 0.06$
7.00	10.00	60	43	5	2310	$6.88 \pm 0.05$	$10.66 \pm 0.14$	2.00	$0.90 \pm 0.09$
7.00	10.00	60	43	5	2307	$6.88 \pm 0.05$	$10.66 \pm 0.14$	2.00	$1.11 \pm 0.08$
7.00	10.00	60	43	5	2306	$6.88 \pm 0.05$	$10.67 \pm 0.14$	2.00	$0.96 \pm 0.09$
7.00	12.50	60	43	5	3396	$6.89 \pm 0.05$	$13.78 \pm 0.18$	2.00	$0.87 \pm 0.05$
7.00	12.50	60	43	5	3395	$6.88 \pm 0.05$	$13.79 \pm 0.18$	2.00	$0.89 \pm 0.07$
7.00	12.50	60	43	5	3401	$6.88 \pm 0.05$	$13.81 \pm 0.18$	2.00	$1.15 \pm 0.14$
7.00	12.50	60	43	5	3402	$6.89 \pm 0.05$	$13.80 \pm 0.18$	2.00	$1.08 \pm 0.13$
7.00	12.50	60	43	5	3395	$6.88 \pm 0.05$	$13.79 \pm 0.18$	2.00	$0.94 \pm 0.15$
7.00	12.50	60	43	5	3401	$6.89 \pm 0.05$	$13.80 \pm 0.18$	2.00	$1.18 \pm 0.04$
7.00	15.00	60	43	5	4521	$6.89 \pm 0.05$	$17.01 \pm 0.22$	2.00	$0.93 \pm 0.09$
7.00	15.00	60	43	5	4520	$6.88 \pm 0.05$	$17.03 \pm 0.22$	2.00	$1.01 \pm 0.08$
7.00	15.00	60	43	5	4514	$6.88 \pm 0.05$	$17.03 \pm 0.23$	2.00	$1.01 \pm 0.07$
7.00	15.00	60	43	5	4517	$6.89 \pm 0.05$	$17.00 \pm 0.22$	2.00	$0.92 \pm 0.09$
7.00	15.00	60	43	5	4518	$6.88 \pm 0.05$	$17.02 \pm 0.22$	2.00	$0.87 \pm 0.06$
7.00	15.00	60	43	5	4520	$6.89 \pm 0.05$	$17.01 \pm 0.22$	2.00	$0.90 \pm 0.07$
7.00	17.50	60	43	5	5628	$6.88 \pm 0.05$	$20.21 \pm 0.26$	2.00	$1.13 \pm 0.10$
7.00	17.50	60	43	5	5622	$6.88 \pm 0.05$	$20.19 \pm 0.27$	2.00	$1.03 \pm 0.11$
7.00	17.50	60	43	5	5627	$6.89 \pm 0.05$	$20.20 \pm 0.27$	2.00	$0.99 \pm 0.07$
7.00	17.50	60	43	5	5624	$6.88 \pm 0.05$	$20.20 \pm 0.27$	2.00	$0.85 \pm 0.12$
7.00	17.50	60	43	5	5628	$6.88 \pm 0.05$	$20.21 \pm 0.27$	2.00	$0.74 \pm 0.04$
7.00	17.50	60	43	5	5627	$6.88 \pm 0.05$	$20.20 \pm 0.27$	2.00	$0.98 \pm 0.12$
7.00	20.00	60	43	5	6725	$6.89 \pm 0.05$	$23.36 \pm 0.30$	2.00	$1.03 \pm 0.09$
7.00	20.00	60	43	5	6730	$6.89 \pm 0.05$	$23.36 \pm 0.31$	2.00	$0.95 \pm 0.07$
7.00	20.00	60	43	5	6730	$6.89 \pm 0.05$	$23.38 \pm 0.31$	2.00	$1.02 \pm 0.11$
7.00	20.00	60	43	5	6727	$6.89 \pm 0.05$	$23.37 \pm 0.31$	2.00	$0.78 \pm 0.06$
7.00	20.00	60	43	5	6730	$6.89 \pm 0.05$	$23.35 \pm 0.31$	2.00	$1.09 \pm 0.08$
7.00	20.00	60	43	5	6726	$6.88 \pm 0.05$	$23.37 \pm 0.31$	2.00	$0.87 \pm 0.07$

Table 4: Simulation details of the constant-density simulations (from previous work<sup>2</sup>) and the corresponding height study (new).

initial width [nm]	initial height [nm]	number ANT1	number POPC	number POPE	number card.	number water	average width [nm]	average height [nm]	simulation time [μs]	rotational diffusion coefficient [rad <sup>2</sup> /μs]
12.0	10.0	1	220	160	20	6588	12.05 ± 0.05	10.19 ± 0.09	2.00	1.34 ± 0.07
24.0	10.0	4	880	640	80	26332	24.10 ± 0.05	10.19 ± 0.04	2.00	1.42 ± 0.03
36.0	10.0	9	1980	1440	180	59202	36.15 ± 0.05	10.18 ± 0.03	2.00	1.39 ± 0.03
48.0	10.0	16	3520	2560	320	105440	48.20 ± 0.05	10.19 ± 0.02	2.00	1.41 ± 0.03
60.0	10.0	25	5500	4000	500	164875	60.24 ± 0.05	10.20 ± 0.02	2.00	1.46 ± 0.04
72.0	10.0	49	10780	7840	980	322812	84.34 ± 0.05	10.19 ± 0.01	2.00	1.49 ± 0.02
120.0	10.0	100	22000	16000	2000	658400	120.48 ± 0.06	10.19 ± 0.01	2.00	1.50 ± 0.02
180.0	10.0	225	49500	36000	4500	1480950	180.72 ± 0.06	10.19 ± 0.01	2.00	1.47 ± 0.02
240.0	10.0	400	88000	64000	8000	2634800	240.96 ± 0.06	10.19 ± 0.01	2.00	1.47 ± 0.02
300.0	10.0	625	137500	100000	12500	4111250	301.20 ± 0.07	10.18 ± 0.00	2.00	1.47 ± 0.02
360.0	10.0	900	198000	144000	18000	5925600	361.45 ± 0.08	10.19 ± 0.00	2.00	1.46 ± 0.02
48.0	7.5	16	3520	2560	320	50272	48.11 ± 0.05	6.97 ± 0.01	2.00	1.49 ± 0.03
48.0	8.5	16	3520	2560	320	70752	48.16 ± 0.05	8.17 ± 0.02	2.00	1.46 ± 0.04
48.0	10.0	16	3520	2560	320	105440	48.20 ± 0.05	10.19 ± 0.02	2.00	1.41 ± 0.03
48.0	12.5	16	3520	2560	320	125040	48.20 ± 0.05	11.34 ± 0.02	2.00	1.44 ± 0.05
48.0	15.0	16	3520	2560	320	153776	48.21 ± 0.05	13.03 ± 0.03	2.00	1.48 ± 0.04

Table 5: Simulation details of the CNT-porin simulations (same setup as in earlier work<sup>3</sup>).

number POPC	number water	average width [nm]	average height [nm]	simulation time [μs]	rotational diffusion coefficient [rad <sup>2</sup> /μs]
58	3061	4.07 ± 0.04	10.22 ± 0.20	0.44	0.65 ± 0.09
115	5497	5.76 ± 0.05	9.38 ± 0.17	0.36	0.88 ± 0.20
153	6078	6.75 ± 0.06	8.23 ± 0.14	0.29	0.69 ± 0.19
188	8732	7.45 ± 0.06	8.98 ± 0.13	0.44	0.95 ± 0.18
277	12499	9.14 ± 0.07	8.64 ± 0.13	0.25	0.83 ± 0.22
437	19579	11.52 ± 0.06	8.51 ± 0.09	0.28	0.76 ± 0.18
785	34922	15.44 ± 0.06	8.45 ± 0.06	0.19	0.80 ± 0.13

## References

- (1) Grønbech-Jensen, N. Summation of Logarithmic Interactions in Nonrectangular Periodic Media. *Comput. Phys. Comm.* **1999**, *119*, 115–121.
- (2) Vögele, M.; Köfinger, J.; Hummer, G. Hydrodynamics of Diffusion in Lipid Membrane Simulations. *Phys. Rev. Lett.* **2018**, *120*, 268104.
- (3) Vögele, M.; Köfinger, J.; Hummer, G. Molecular Dynamics Simulations of Carbon Nanotube Porins in Lipid Bilayers. *Faraday Discuss.* **2018**, *209*, 341–358.